XLI CILAMCE
XLI Ibero-Latin American Congress on Computational Methods in Engineering
16-19 November, 2020 FOZ DO IGUAÇU PARANÁ - BRAZIL

Proper Generalized Decomposition (PGD) applied to heat conduction problem in heterogeneous materials

Paulo de Tarso R. Mendonça[1], Vinícius Gregory Gonçalves[1],

[1]*Dept. of Mechanical Engineering, Federal Universirty of Santa Catarina*
R. Lauro Linhares, 1850 - Trindade, 88070-260, Florianópolis, Santa Catarina, Brazil
mendonca@grante.ufsc.br, viniciusgregorygo@gmail.com

Abstract. In order to reduce processing time in complex simulations, several order reduction methods have been developed. One of these methods is the Proper Generalized Decomposition (PGD). The PGD method is based on the decomposition of unknown fields in each of the coordinates. PGD is used to solve sequences of one-dimensional problems of the finite element method. Throughout the iterations, the spatial variables are separated via the PGD method, resulting in an iterative sequence of global solutions, even in a linear problem. The present work aims to evaluate the PGD method in heat conduction problems using heterogeneous materials.

Keywords: Proper Generalized Decomposition (PGD), Heat Conduction, Heterogeneous Materials.

1 Introducion

The focus of this work will be the Proper Generalized Decomposition (PGD) a priori order reduction model, as presented in the work of Chinesta et al. [1]. This method consists of building a reduced base without prior knowledge, a priori, of the solution. Basically, a PGD approximation of the solution is constructed by successive enrichment. This enrichment is done in the form of a finite sum of N functional products, involving the functions of each coordinate, as shown in the work of Badías et al. [2] and Huerta et al. [3].

So, this article describes the formulations developed to obtain approximate solutions to the problem of heat conduction in heterogeneous materials. As already mentioned, the PGD method will be used, which consists of obtaining the solution by a sequence of unidimensional problems of the Finite Element Method (MEF), as shown in the work of Bognet et al. [4] and Chinesta and Ladevèze [5]. PGD is based on separated decomposition of the unknown field in each of their coordinates, reducing the computational efforts in several orders of magnitude, as presented by Chinesta and Ladevèze [5] and Ammar [6]. The method involves an iterative sequence of global solutions even in a linear problem Nouy [7] and Ammar [6]. However, previous experiences in the literature shows that the number of iterations and modes is small, and the total computational cost involved is generally smaller than the cost of the single 2D or 3D analysis by finite elements model González et al. [8], Ammar [6] and Chinesta et al. [9].

The PGD is based on the separation of the unknown field in each of the coordinates. It has been used in the space-time decomposition of parabolic problems as in the works of Boucinha et al. [10], Nouy [11], reducing computational efforts by several orders of magnitude. In the work of Boucinha et al. [10], a PGD formulation is developed for second order hyperbolic differential equations, with an emphasis on transient and tested elasto-dynamics models for problems with a dimension in space (bar) and time. The PGD solution process can follow several strategies, because the algebraic system is always non-linear. In this work, we consider only the problem of heat conduction in steady state.

The text develops formulations for two complementary problems as described in Bognet et al. [4]. First, we present the formulation for the heat conduction problem in a regular representative volume (RVE), where all data are represented by their adequate PGD modes. Second, a PGD formulation is developed to obtain a PGD description of the highly oscillatory material property data, for example thermal conductivity (or elastic modulus, thermal source, heat flux at a region of the boundary, compression forces). This description is composed by a sequence of discrete modes uncoupled in each of the three cartesian coordinates, and are used in the first part of the formulation.

The objective of this work is to evaluate the quality of the approximation response obtained by the PGD

method in comparison with the MEF, since PGD offers the benefit of saving computational time, which is an important factor for multidimensional problems.

2 Proper Generalized Decomposition (PGD) for the heat conduction problem

The formulation described here generalizes the ideas explored in Bognet et al. [4] and the formulation is developed for a 3D domain, but the computational implementation and results are obtained to 2D domain. Let us initially consider a body, subject to adequate sources and boundary conditions, with the geometric form of a regular volume Ω with dimensions $\Omega = L_x \times L_y \times L_z$ along the cartesian coordinates $\mathbf{x} = (x, y, z)$. The boundary Γ of the body is composed by the six faces designated as $\Gamma_1, \Gamma_2, \cdots, \Gamma_6$, where Γ_1 and Γ_2 have normals in $-x$ and $+x$ axis, Γ_3 and Γ_4 have normals in $-y$ and $+y$ axis, Γ_5 and Γ_6 have normals in $-z$ and $+z$ axis. Here we consider the strong form for steady state heat flux and homogeneous and istropic material

$$\begin{aligned} \nabla \cdot (\mathbf{k}\nabla\theta) &= -b, \quad \text{for } \mathbf{x} \in \Omega, \\ \theta(\mathbf{x}) &= \bar{T}(\mathbf{x}), \quad \text{for } \mathbf{x} \in \Gamma_u, \\ q(\mathbf{x}) &= (\mathbf{k}\nabla\theta)\cdot\mathbf{n} = h(\mathbf{x}), \quad \text{for } \mathbf{x} \in \Gamma_q. \end{aligned} \tag{1}$$

where k is thermal conductivity, b is heat source, $\bar{T}(\mathbf{x})$ and $h(\mathbf{x})$ are temperature and heat flux prescribed on parts of the boundary, respectively. We consider a decomposition of the temperature field as

$$\begin{aligned} \theta(\mathbf{x}) &= T(\mathbf{x}) + G(\mathbf{x}), \text{ for } \mathbf{x} \in \Omega, \text{ where} \\ T(\mathbf{x}) &= 0 \quad \text{for } \mathbf{x} \in \Gamma_u, \\ G(\mathbf{x}) &= \bar{T}(\mathbf{x}), \quad \text{for } \mathbf{x} \in \Gamma_u, \end{aligned} \tag{2}$$

This decomposition of the temperature fields and adequate manipulations generates the following weak form: given $G \in Kin$, find $T \in Var$,

$$\int_\Omega \nabla\hat{u}\cdot(\mathbf{k}\nabla T)\ d\Omega = \int_\Omega \hat{u}b\ d\Omega + \int_{\Gamma_q} \hat{u}h\ d\Gamma - \int_\Omega \nabla\hat{u}\cdot(\mathbf{k}\nabla G)\ d\Omega, \quad \text{for } \forall\hat{u} \in Var, \tag{3}$$

where the sets of solution and of variations are equals: $Kin = Var = \left\{ f \in H^1(\Omega), \text{ such that, } f(\mathbf{x}) = 0\ \forall\hat{u} \in Var \right\}$.

Consider available the PGD representation of thermal conductivity as $k(\mathbf{x}) = \sum_{l=1}^{nk} D_l k_{xl}(x) k_{yl}(y) k_{zl}(z)$, and and heat source as $b(\mathbf{x}) = \sum_{j=1}^{nb} L_j b_{xj}(x) b_{yj}(y) b_{zj}(z)$, where nk and nb are PGD modes necessary to represent thermal conductivity and heat source, respectively. Let us consider that there are already available nu PGD modes, and we seek the next mode $T_{nu+1}(\mathbf{x})$. Thus, we have the following representation with variation separation:

$$T(\mathbf{x}) = \underbrace{\sum_{m=1}^{nu} T_{xm}(x)T_{ym}(y)T_{zm}(z)}_{T_0(\mathbf{x})} + \underbrace{T_x(x)T_y(y)T_z(z)}_{T_{nu+1}(\mathbf{x})}, \text{ that is, } T(\mathbf{x}) = T_0(\mathbf{x}) + T_{nu+1}(\mathbf{x}). \tag{4}$$

where $T_0(\mathbf{x})$ is known and we seek $T_{nu+1}(\mathbf{x})$. We proceed to a spacial discretization for $T_{nu}(\mathbf{x})$:

$$T_x(x) = \sum_{p=1}^{px} T_{xp}\phi_{xp}(x) = \Phi_x(x)\mathbf{T}_x, \quad \text{for } x \in [0, L_x],\ \forall\ T_x(x) \in Var_x, \tag{5}$$

where the space is

$$Var_x = \left\{ f \in H^1(\Omega_x), \text{such that } f(x) = 0 \text{ for all } x \in \Gamma_x \right\}. \tag{6}$$

Similarly, we have the spacial discretizations and the spaces for directions y and z. The domain and boundary are: for x $\Omega_x(0, L_x)$ and Γ_x $\{0, L_x\}$, for y $\Omega_y(0, L_y)$ and Γ_y $\{0, L_y\}$ and for z $\Omega_z(0, L_z)$ and Γ_z $\{0, L_z\}$. Each

set of functions $\phi_{xp}(x)$, $\phi_{yp}(y)$ and $\phi_{zp}(z)$ is a set of piecewise continuous finite element basis functions, one-dimensional, associated with a given mesh in x, y or z directions, and $\mathbf{T}_x$, $\mathbf{T}_y$ and $\mathbf{T}_z$, are unknown nodal coefficients for the $nu+1$-th PGD mode of the temperature, in the meshes of x, y, z directions, respectively. These are the coefficients that generate the virtual mesh, similar to the finite element generated mesh. In the present formulation, $T_x(x) \in Var_x$ but not all basis component $\phi_{xp}(x)$ are required to belong to Var_x. Nodes p span the entire domain $\bar{\Omega}_x$. Thus, the condition $T_x(x)=0$ on $x \in \Gamma_x$ is satisfied adjusting the adequate nodal value in $\mathbf{T}_x$ and in its variation $\hat{\mathbf{T}}_x$. The same holds for $\phi_{yp}(y)$ and $\phi_{zp}(z)$. The temperature gradient is discretized by

$$\begin{aligned} \nabla T &= \nabla T_0 + \nabla T_n, \text{ i.e.,} \\ \nabla T &= \nabla T_0 + \left\{ \begin{array}{l} (\Phi_{x,x}\mathbf{T}_x)\,(\Phi_y\mathbf{T}_y)\,(\Phi_z\mathbf{T}_z) \\ (\Phi_x\mathbf{T}_x)\,(\Phi_{y,y}\mathbf{T}_y)\,(\Phi_z\mathbf{T}_z) \\ (\Phi_x\mathbf{T}_x)\,(\Phi_y\mathbf{T}_y)\,(\Phi_{z,z}\mathbf{T}_z) \end{array} \right\}. \end{aligned} \tag{7}$$

The variation of the temperature is $\hat{T}(\mathbf{x}) = \hat{T}_n(\mathbf{x}) = \hat{T}_x T_y T_z + T_x \hat{T}_y T_z + T_x T_y \hat{T}_z$,

Weak forms

Case only $\hat{T}_x \neq 0$, given T_y and T_z. From eq. (4), the approximate temperature and the gradient at the new mode $nu+1$ is in the form:

$$\begin{aligned} \hat{T}(\mathbf{x}) &= \hat{T}_n(\mathbf{x}) = \hat{T}_x T_y T_z = \left[T_y T_z \Phi_x\right]_{1\times P_x} \hat{\mathbf{T}}_x = \mathbf{N}_x \hat{\mathbf{T}}_x, \\ \delta\nabla T &= \left[\begin{array}{l} T_y T_z \Phi_{x,x} \\ T_{y,y} T_z \Phi_x \\ T_y T_{z,z} \Phi_x \end{array} \right]_{3\times P_x} \hat{\mathbf{T}}_x = \mathbf{B}_x \hat{\mathbf{T}}_x. \end{aligned} \tag{8}$$

where $T_{y,y} = \Phi_{y,y}\mathbf{T}_y$, $T_{z,z} = \Phi_{z,z}\mathbf{T}_z$ and P_x is number of nodes in the direction x. The approximate weak form becomes

$$\begin{aligned} \hat{\mathbf{T}}_x^T \left(\int_\Omega k \mathbf{B}_x^T \mathbf{B}_x d\Omega \right) \mathbf{T}_x = \hat{\mathbf{T}}_x^T \Bigg(& \int_\Omega \mathbf{N}_x^T b \; d\Omega \; + \int_{\Gamma_q} \mathbf{N}_x^T h \; d\Omega - \\ & \int_\Omega k \mathbf{B}_x^T \nabla T_0 d\Omega - \int_\Omega k \mathbf{B}_x^T \nabla G d\Omega \Bigg), \end{aligned} \tag{9}$$

that is, $\mathbf{K}_x \mathbf{T}_x = \mathbf{F}_x$, where $\mathbf{K}_x$ has dimension $P_x \times P_x$.

We can use these expression analogously to $\hat{T}_y \neq 0$ and $\hat{T}_z \neq 0$.

2.1 PGD Representation of scalar data

PGD can be used to represent scalar data, like a material scalar property (thermal conductivity component $k_{ij}(\mathbf{x})$, or elastic modulus component $E_{ij}(\mathbf{x})$) or a load like thermal source $b(\mathbf{x})$, heat flux at a region of the boundary $h(x)$, etc. This representation is necessary to obtain all integrals in eq. (9) decoupled in x, y and z, that is, we obtain three independent 1D integrals.

To demonstrate how the PGD representation works, let consider the variation on the domain highly oscillatory or random, as in an heterogeneous non-periodical material. Consider a PGD representation for $k(\mathbf{x})$:

$$\tilde{k}(\mathbf{x}) = \underbrace{\sum_{l=1}^{nk} D_l k_{xl}(x) k_{yl}(y) k_{zl}(z)}_{k_0(\mathbf{x})} + \underbrace{k_x(x) k_y(y) k_z(z)}_{k_n(\mathbf{x})}, \quad \text{that is, } \tilde{k}(\mathbf{x}) = k_0(\mathbf{x}) + k_n(\mathbf{x}). \tag{10}$$

where $k_0(\mathbf{x})$ is known and we seek $k_n(\mathbf{x})$. In the first step, $k_0(\mathbf{x})$ is absent. We define a squared error functional

as $E(k_x, k_y, k_z) = \int_\Omega \left[k(\mathbf{x}) - (k_0 + k_x k_y k_z)\right]^2 \, d\Omega$, where $k(\mathbf{x})$ is the given data of the property. The variation of the error functional for direction x is

$$\delta E_x(k_x, k_y, k_z) \quad = \quad \frac{\partial E}{\partial k_x}\delta k_x = 2\int_\Omega \left[k(\mathbf{x}) - \tilde{k}\right] \delta k_x k_y k_z \, d\Omega = 0. \tag{11}$$

We proceed to a spacial discretization for $k_n(\mathbf{x})$:

$$k_x(x) \quad = \quad \sum_{p=1}^{nx} Q_{xp}\phi_{xp}(x) = \Phi_x(x)\mathbf{Q}_x, \tag{12}$$

where $\mathbf{Q}_x$ is column vectors of nodal values of the approximation. eq. (11) gives

$$\int_\Omega \left[k(\mathbf{x}) - k_0\right] k_y k_z \delta k_x \, d\Omega = \int_\Omega k_x k_y^2 k_z^2 \delta k_x \, d\Omega. \tag{13}$$

The variation δk_x is represented from eq. (12) $\delta k_x = \mathbf{\Phi}_x(x)\hat{\mathbf{Q}}_x$. Thus, (13) becomes

$$\hat{\mathbf{Q}}_x^T \underbrace{\int_\Omega \mathbf{\Phi}_x^T \left[k(\mathbf{x}) - k_0\right] k_y k_z \, d\Omega}_{\mathbf{F}_x} = \hat{\mathbf{Q}}_x^T \underbrace{\left[\int_x \mathbf{\Phi}_x^T \mathbf{\Phi}_x dx \int_y k_y^2 dy \int_z k_z^2 \, dz\right]}_{\mathbf{K}_x} \mathbf{Q}_x, \tag{14}$$

$$\mathbf{K}_x \mathbf{Q}_x = \mathbf{F}_x, \tag{15}$$

where $\mathbf{K}_x$ is a symmetric mass-like matrix, which is obtained from three independent 1D integrals. However, at this point, $\mathbf{F}_x$ requires coupled integration in all three dimensions, due to the physical data $k(\mathbf{x})$. Analogously, we obtain y and z systems: $\mathbf{K}_y\mathbf{Q}_y = \mathbf{F}_y$ and $\mathbf{K}_z\mathbf{Q}_z = \mathbf{F}_z$. Algebraic system eq. (15) is coupled and non-linear.

The force term in eq. (14) can be decomposed using the PGD separated representation of k_0 in eq. (10)

$$\begin{aligned}
\mathbf{F}_x \quad &= \quad \int_\Omega \mathbf{\Phi}_x^T \left[k(\mathbf{x}) - k_0\right] k_y k_z \, d\Omega, \\
&= \quad \int_\Omega \mathbf{\Phi}_x^T k(\mathbf{x}) k_y k_z \, d\Omega - \sum_{l=1}^{nk} D_l \left(\int_x \mathbf{\Phi}_x^T k_{xl} \, dx\right)\left(\int_y k_{yl} k_y dy\right)\left(\int_z k_{zl} k_z \, dz\right), \\
&= \quad \mathbf{F}_x^k - \mathbf{F}_x^0.
\end{aligned} \tag{16}$$

Analogously to obtain $\mathbf{F}_y = \mathbf{F}_y^k - \mathbf{F}_y^0$ and $\mathbf{F}_z = \mathbf{F}_z^k - \mathbf{F}_z^0$

Therefore, the parts $\mathbf{F}_x^0$, $\mathbf{F}_y^0$ and $\mathbf{F}_z^0$ can be integrated separately in each direction, and only $\mathbf{F}_x^k$, $\mathbf{F}_y^k$ and $\mathbf{F}_z^k$ must be integrated in coupled form because the term $k(\mathbf{x})$.

2.2 Heterogeneous materials (Two phases materials)

Consider the heterogeneous material constituted by two or more materials, where the matrix property is k^m and the inclusions of property is k^i. Both, matrix and inclusions, are considered isotropic homogeneous. Consider the property of the inclusion be decomposed as $k^i = k^m + \Delta k$. Thus, $\mathbf{F}_x^k = \int_\Omega \mathbf{\Phi}_x^T k(\mathbf{x}) k_y k_z \, d\Omega$ of eq. (16) becomes $\mathbf{F}_x^k = k^m \int_\Omega \mathbf{\Phi}_x^T k_y k_z \, d\Omega + \Delta k \int_{\Omega_i} \mathbf{\Phi}_x^T k_y k_z \, d\Omega$, where Ω_i is the union of the inclusion domains. k^m is a constant in Ω and ΔK is constant in every inclusion. If the inclusion is cubic with faces parallel to the coordinate axes, both integrals can be uncoupled in the cartesian directions:

$$\mathbf{F}_x^k = k^m \int_x \mathbf{\Phi}_x^T \, dx \int_y k_y \, dy \int_z k_z \, dz + \Delta k \sum_{p=1}^{ni} \int_{x\in\Omega_p} \mathbf{\Phi}_x^T dx \int_{y\in\Omega_p} k_y dy \int_{z\in\Omega_p} k_z dz \tag{17}$$

n_i is the number of inclusions and Ω_p is the domain of the p-th inclusion. Analogously to obtain $\mathbf{F}_y^k$ and $\mathbf{F}_z^k$

All tests for PGD representation were realized considering the integrals uncoupled in the cartesian directions, that is, all inclusions are cubic with faces parallels to the coordinates axes.

3 Results

The problems will be dealt with in a 2D domain. To test the methodology, the PGD method was tested cases with analytical solutions and with two or more phases of material, as showed in Sec. 2.2. In case with more phases, one of the cases handled uses a 10×10 meters domain, where the matrix has a constant thermal conductivity $k^m = 0.5$ W/(mºC) and have two others materials, as inclusions, $k^A = 1.0$ W/(mºC) and $k^B = 2.0$ W/(mºC). The material k^A (light blue) occupies 15% of the total area and k^B (red) occupies 10%, totalling 25% of the total area occupied by inclusions, as showed in Fig. 1. The Table 1 shows the Norm L_2 of the temperature

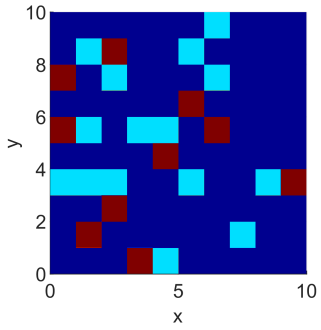

Figure 1. Material configuration and arrangement of inclusions.

of the results obtained with the FEM and PGD methods, varying the number of nodes ($nned$) in each directions and the number of modes PGD (M), and also the relative error between the Norm L_2 solutions. The Fig. 2 shows the behaviour of the temperature and heat flux in the directions x along the line $y = 3.0$ m using 25 modes.

Table 1. Norm L_2 of the temperature of the problem varying the number of nodes in each direction ($nned$), using 2 modes ($2M$), 10 modes ($10M$) and 25 modes ($25M$). The relative error between the solution of FEM and PGD methods are shown too.

	Temperature Norm L_2				Relative temperature error (%) - FEM × PGD		
$nned$	FEM	PGD $2M$	PGD $10M$	PGD $25M$	PGD $2M$	PGD $10M$	PGD $25M$
11	62.7449	54.9860	55.9549	56.5134	12.3658	10.8215	9.9316
51	63.0756	59.8042	60.4221	61.0978	5.1864	4.2068	3.1355
101	63.1108	58.5556	58.8542	60.1185	7.2178	6.7446	4.7413
201	63.1252	58.6672	58.8776	59.2256	7.0621	6.7289	6.1775
501	63.1319	58.6204	60.0395	60.0618	7.1461	4.8983	4.8631
1001	63.1336	58.6876	59.6380	59.9563	7.0420	5.5368	5.0327
1251	63.1339	58.0307	60.1653	60.3796	8.0830	4.7021	4.3626

It is observed how the relative error between the norms of the results obtained via FEM and PGD decreases as more modes are added, but the addition of more nodes did not imply a decrease in the relative error. For example, the relative error using 2 modes and 51 nned is less than the relative error using 2 modes and 1251 nned. This fact can also be observed using 10 and 25 modes and it happens due to the dependence of the PGD method on the number of nodes used in each direction, as it directly implies the coefficients used to generate the nodal values of the virtual mesh.

It can be seen in Fig. 2 how the behaviour of the PGD method with respect to the heat flow in the x direction shows greater discrepancy when compared to the FEM method. Fig. 3 shows the results obtained with the FEM and PGD method in the entire domain and the absolute error between the two solutions in the entire domain, where it becomes more evident that the PGD method approach presents greater errors with respect to heat flow, both in

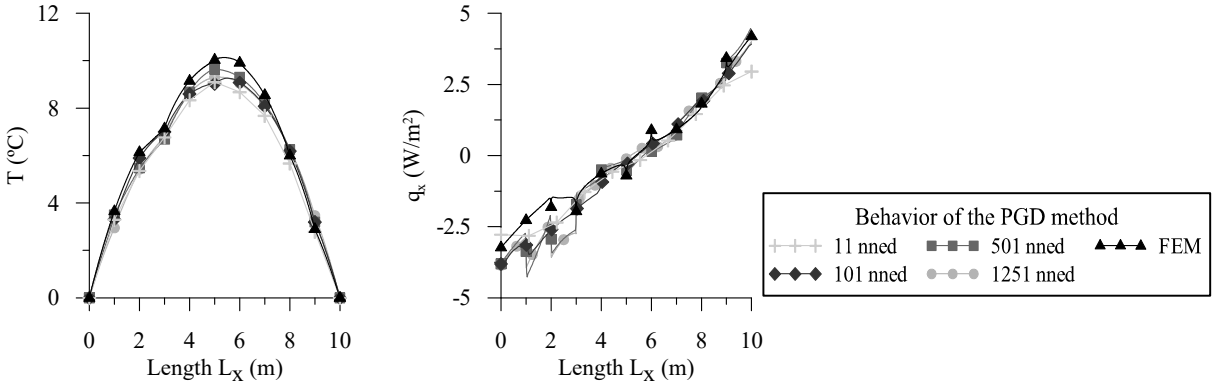

Figure 2. Behaviour of the temperature and heat flux in the direction x along the line $y = 3.0$ m using 25 modes.

the x and y directions. This happens because the temperature is obtained directly by the approached method, while the heat flow is a derivative of the temperature, thus causing a larger error in the response of numerical method. The PGD solution is Fig. 3 was generated using 501 nodes in each direction and 25 modes.

In this case, using PGD approximation, we can several times less processing. This means, using 501 nned and 25 modes, we have $(501 + 501) \times 25 = 25050$ ndof and the traditional FEM we have $501^2 = 251001$ ndof.

4 Conclusion

The numerical examples covered in this work are simple, of a numerical nature and were approached without practical interest, as the objective was to analyse the potential of PGD as an alternative method of solving the heat conduction problem.

Using the PGD approach described in this article, we conclude that this method is capable of representing the problem addressed efficiently. In addition, using the proposed method, it is possible to save a lot of processing time compared to the traditional finite element method, as seen in the example discussed. Thermal conductivity was used as a target, but the same technique can be used for other data necessary to model the heat conduction problem, such as the heat source, temperature and heat flow prescribed in the contour, etc.

It is important to show the importance of representing the material as presented in Sec. 2.1, as this artifice is necessary to be able to integrate Eq. 9, for direction x, and analogously to y and z.

Acknowledgements. The authors would like to thank the financial support provided by the Brazilian funding agencies CAPES - (Coordination for the Improvement of High Education Personnel) and CNPq - (National Council for Scientific and Technological Development).

Authorship statement. The authors hereby confirm that they are the sole liable persons responsible for the authorship of this work, and that all material that has been herein included as part of the present paper is either the property (and authorship) of the authors, or has the permission of the owners to be included here.

References

[1] Chinesta, F., Ladeveze, P., & Cueto, E., 2011. A short review on model order reduction based on proper generalized decomposition. *Archives of Computational Methods in Engineering*, vol. 18, n. 4, pp. 395.

[2] Badías, A., González, D., Alfaro, I., Chinesta, F., & Cueto, E., 2017. Local proper generalized decomposition. *International Journal for Numerical Methods in Engineering*, vol. 112, n. 12, pp. 1715–1732.

[3] Huerta, A., Nadal, E., & Chinesta, F., 2018. Proper generalized decomposition solutions within a domain decomposition strategy. *International Journal for Numerical Methods in Engineering*, vol. 113, n. 13, pp. 1972–1994.

[4] Bognet, B., Bordeu, F., Chinesta, F., Leygue, A., & Poitou, A., 2012. Advanced simulation of models defined in plate geometries: 3d solutions with 2d computational complexity. *Computer Methods in Applied Mechanics and Engineering*, vol. 201, pp. 1–12.

[5] Chinesta, F. & Ladevèze, P., 2014. Separated representations and pgd-based model reduction. *Fundamentals and Applications, International Centre for Mechanical Siences, Courses and Lectures*, vol. 554, pp. 24.
[6] Ammar, A., 2010. The proper generalized decomposition: a powerful tool for model reduction. *International Journal of Material Forming*, vol. 3, n. 2, pp. 89–102.
[7] Nouy, A., 2010a. A priori model reduction through proper generalized decomposition for solving time-dependent partial differential equations. *Computer Methods in Applied Mechanics and Engineering*, vol. 199, n. 23-24, pp. 1603–1626.
[8] González, D., Ammar, A., Chinesta, F., & Cueto, E., 2010. Recent advances on the use of separated representations. *International Journal for Numerical Methods in Engineering*, vol. 81, n. 5, pp. 637–659.
[9] Chinesta, F., Keunings, R., & Leygue, A., 2013. *The proper generalized decomposition for advanced numerical simulations: a primer*. Springer Science & Business Media.
[10] Boucinha, L., Gravouil, A., & Ammar, A., 2013. Space-time proper generalized decompositions for the resolution of transient elastodynamic models. *Computer Methods in Applied Mechanics and Engineering*, vol. 255, pp. 67–88.
[11] Nouy, A., 2010b. A priori model reduction through proper generalized decomposition for solving time-dependent partial differential equations. *Computer Methods in Applied Mechanics and Engineering*, vol. 199, n. 23-24, pp. 1603–1626.

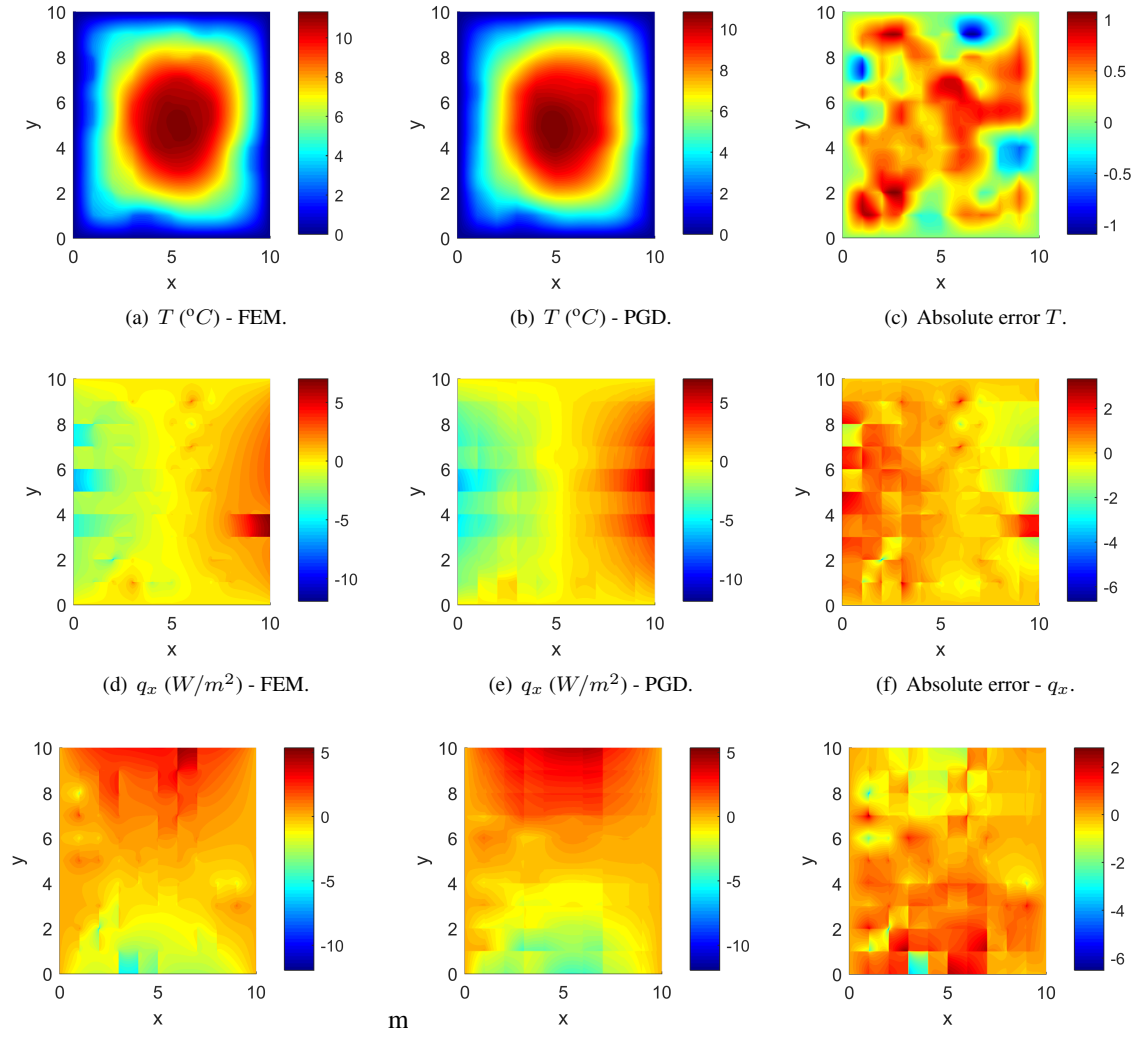

Figure 3. Solutions using FEM and PGD (501 nned and 25 modes) in 2D visualization and absolute error between FEM and PGD solutions in all the domain.